

Cross section of the process $e^+ + e^- \rightarrow \Xi^0 + \bar{\Xi}^0$ including three-gluon and D -meson loop contributions

Azad I. Ahmadov^{a,b} *

^a *Institute of Physics, Ministry of Science and Education,*

H.Javid avenue, 131, AZ1143 Baku, Azerbaijan and

^b *Bogoliubov Laboratory of Theoretical Physics, JINR, Dubna, 141980 Russia*

(Dated: July 8, 2025)

arXiv:2507.04835v1 [hep-ph] 7 Jul 2025

* E-mail: ahmadov@theor.jinr.ru

Abstract

In this paper, we investigate the production of a $\Xi^0\bar{\Xi}^0$ using e^+e^- collision data at ten center-of-mass energies between 3.51 and 4.95 GeV collected with the BESIII detector at the BEPCII collider and corresponding to an integrated luminosity of 30 fb^{-1} to study the structure of baryons. The data collected by the BESIII detector are useful for the study of XYZ states, and this collaboration continues the exploration of these exotic charmonium-like states. The study of the baryon-antibaryon pair production at the electron-positron linear collider is of fundamental interest in studying of the basic structure of the Standard Model and studying their production gives a unique insight into their structure. Moreover, that at higher center-of-mass energies the baryon-antibaryon pair production in electron-positron annihilation provides a powerful tool. We explore a hyperon pair produced in the electron-positron annihilation reactions. In the present paper we present the phenomenological results of our studies on the production of $\Xi^0\bar{\Xi}^0$ in e^+e^- annihilation at the BESIII detector at the BEPCII Collider. In the reaction $e^+e^- \rightarrow \Xi^0\bar{\Xi}^0$, we consider two different contributions: one from the D meson loop and the other from the three-gluon charmonium annihilation. We compute the total cross section of the process $e^+e^- \rightarrow \Xi^0\bar{\Xi}^0$ including the contributions of the D -meson loop and three-gluon loops as well as the interference of all diagrams. As for the purely electromagnetic mechanism, large relative phases are generated for these contributions. For a large momentum transferred region we get as a byproduct a fit of the electromagnetic form factor of the Ξ^0 - hyperon. In this paper, in addition to the $\psi(3770)$ charmonium, we also take into account the contributions of other charmonium (-like) states, such as $\psi(4040)$, $\psi(4160)$, $Y(4230)$, $Y(4360)$, $\psi(4415)$, and $Y(4660)$. On the whole our results are in good agreement with the available experimental data.

PACS numbers: 12.38.Qk, 12.20.-m, 13.25.Gv, 12.38.Bx, 13.66.Bc, 13.40.Gp, 14.20.Jn, 12.38.-t

Keywords: Ξ^0 Hyperon, Born cross section, charmonium production, charmoniumlike states, D -meson loop mechanism, three gluon mechanism, Form Factor

I. INTRODUCTION

We understand that the study of the processes of annihilation of colliding electron-positron beams and inelastic lepton-nucleon scattering has played a significant role in the development of modern elementary particle physics. Most of the phenomena and whole families of hadron resonances ψ and Υ were discovered precisely in these experiments, which play an important role in understanding the nature of fundamental interactions and the structure of elementary particles.

In the physics of the microworld, one of the main problems is the confirmation of the Standard Model (SM) [1–4] and the search for possible exits beyond its limits in order to obtain effective results at colliders and accelerators. We know that particle physics is constantly searching for the most fundamental method for describing matter and forces. From this point of view, particle physics, using quarks and leptons and their interactions, tries to explain the diversity of the Universe. Therefore, the reactions $e^+e^- \rightarrow \Sigma^0\bar{\Sigma}^0$, $e^+e^- \rightarrow \Sigma^+\bar{\Sigma}^-$, $e^+e^- \rightarrow p\bar{p}$, and $e^+e^- \rightarrow \Xi^0\bar{\Xi}^0$ are among the main processes studied at electron-positron colliders.

One of the main sources of fundamental information in elementary particle physics is experiments on electron-positron interactions.

It is necessary to note that the formation of hadrons with a pair of baryons or strange mesons in the final state in e^+e^- annihilation process has been one of the main tasks of experimental study during many years for several reasons. First, they give a significant contribution to the total cross section of e^+e^- hadrons. Second, electromagnetic timelike form factors can be derived from these reactions. Also, but not least, when studying these reactions, new states can be discovered. Let us also note that for quantum chromodynamics (QCD) studies, the hadron production in e^+e^- annihilation is an ideal laboratory. There is no interference with the lepton initial state for final states of hadrons.

It should be noted that experiments with electron-positron interactions have given several interesting results in the vector meson region on the annihilation cross section as well as some preliminary results in the region of several GeV.

Therefore, the production of baryon-antibaryon pairs at the electron-positron linear collider is one of the main subjects for studying the basic structure of the Standard Model. To study the structure of baryons, in this paper we want to investigate the production of a

baryon pair in the e^+e^- annihilation within the framework of the Standard Model.

Note that by creating different states of matter and antimatter, the Standard Model of particle physics describes how quarks interact with each other.

After the discovery of hyperons and the study of the mechanisms of their formation, decay processes became of current interest in hadron physics.

It is known that below the $D\bar{D}$ threshold the spectrum is experimentally and theoretically well understood. We know that with high accuracy the masses and total widths of charmonium states have been widely measured but the decay behavior, especially of states that do not carry quantum numbers $J^{PC} = 1^{--}$, is still incomplete. In such cases, with high accuracy vector states can be easily studied in e^+e^- annihilation in resonant production. Therefore, the BESIII experiment plays a considerable role and offers a good opportunity for the study of these states due to the high-statistics data samples.

The investigation of charm physics plays one of the important roles in understanding and studying the Standard Model.

It is known that using e^+e^- annihilation data taken by the BESIII detector, several searches for charmonium-like states were performed, that is $\psi(4040)$, $\psi(4160)$, $Y(4230)$, $Y(4360)$, $\psi(4415)$, $Y(4660)$ and others.

There were discoveries of many unexpected charmonium-like states, which stimulated renewed interest in charmonium physics. Namely, charmonium spectroscopy has been revived due to the discovery of many new states above the open charm threshold. However, there are more states that observed only in single experiments or only in single decays and, therefore, additional theoretical and experimental data are needed to study these phenomena.

For many years, a number of new hadron states, including charmonium-like XYZ states, have generated extensive discussions about the study of the exotic hadron family [5–11]. Among these observed charmonium-like XYZ states, the ones directly produced in e^+e^- annihilation, which are called Y states, are emphasized in the BESIII Paper [12]. Charmonium production with energies above the threshold is of great theoretical interest due to its richness in $c\bar{c}$ states, the properties of which are still being studied.

Among these new states, $Y(4260)$ [13–15], $Y(4360)$, and $Y(4660)$ [16–19] have quantum numbers $J^{PC} = 1^{--}$ of charmonium-like Y -family states and are formed as a result of the e^+e^- annihilation process.

It is pleasure to note that the BESIII detector at the BEPCII collider has collected very

large data sets. It was reported that some results were obtained on baryon pair production in charmonium(-like) decays, $J/\psi, \psi(2S), \psi(3770)$, etc., and in the positron-electron annihilations, which include the observation of a large number of charmonium modes, the most accurate measurements of the nucleon form factor and more accurate studies of baryon pair production near the threshold. To verify the Standard Model, for example, to discover undisclosed aspects of the description of the structure of hadronic resonances using QCD, these results provide a rich laboratory [20–26].

It can be assumed that charmonium is now interpreted as non-relativistic bound states of charm and anti-charm quarks. Therefore, experimental measurements of charmonium decays may become an ideal laboratory for studying the dynamics of strong interaction physics and testing various aspects of quantum chromodynamics (QCD) [27, 28].

Of course, one of the most basic properties of QCD is its spectrum. After the experimental discovery of entirely new exotic hadronic states in this region, significant progress can be expected in charmonium spectroscopy above the open-charm threshold. The main strength of e^+e^- colliders is that they allow obtaining large data sets by possible at or near the masses of charmonium vector states with the well-known initial state quantum numbers. At present, BESIII is the only experiment that collects data using e^+e^- collisions in the field of charmonium.

We understand that nucleons, despite being the lightest baryons, are the largest component of observable matter in the Universe and have been shown to be non-point particles [29, 30].

It must be emphasized that hyperons are SU(3)-flavor-octet partners of nucleons that contain one or more strange quarks and offer some extra dimensions for exploring nucleon structures [31–35].

Electromagnetic form factors (EMFFs) are used to understand the effects of quantum chromodynamics (QCD) in hadron resonances, which parameterize the internal structure and dynamics of hadrons (hyperons and nucleons) [36–39]. It should be noted that we use time-like EMFFs because they provide fundamental information and describe the modifications of the point-like photon-hadron vertex due to the internal structure and dynamics of hadrons. Time-like EMFFs were measured in the processes $e^+e^- \rightarrow B\bar{B}$ [40–44] (where B denotes the ground baryon state with spin 1/2).

A lot of experimental measurements and theoretical results have shown that charmed

baryons also represent an interesting dynamical system for studying strong and weak interactions.

The electromagnetic structure of hadrons was studied in the original papers of Hofstaedter [45, 46], which remains an open and interesting object of research in high-energy physics. At present, the production of hadrons at high energies in the electron-positron annihilation processes is one of the main tools for studying the structure of the nucleon.

Let us also note that in the Belle experiment, in the study of the ISR process $e^+e^- \rightarrow \eta J/\psi$, only the well-known charmonium states $\psi(4040)$ and $\psi(4160)$ [47] were detected.

Moreover, since the resonance $\psi(3770)$ decays almost entirely into pure $D\bar{D}$ [48], the resonance $\psi(3770)$ is the lowest-mass resonance of charmonium above the open charm pair formation threshold $D\bar{D}$. It should be noted that due to the discovery of many new states above the open charm threshold, charmonium spectroscopy has begun to develop again.

We understand that for the construction of a charmonia family, the vector charmonium-like Y -state plays a special role.

Let us note that in experimental measurements all charmonium states were observed below the mass threshold for charm pairs ($2m_D$), and their observed spectrum was known to be consistent with the charm-anticharm potential model prediction [49].

It should also be noted that two-particle baryon decays of vector ($J^{PC} = 1^{--}$) charmonium (like) resonances, as shown in [50, 51], provide a huge opportunity for predictions of QCD.

To analyze the cross section in the $\bar{p}p \rightarrow e^+e^-$ and $e^+e^- \rightarrow \bar{p}p$ [52] processes in the near-threshold region, the effective form factors (G_E and G_M form factors) for the proton were used, and in the paper [53] it was noted that in the *BABAR* data there are deviations in the existence of proton timelike form factors (FFs) from the pointlike behavior of the $p\bar{p}$ electromagnetic current.

In this letter, we continue the study of baryon time-like EMFFs for the present process.

The cross-section of the process of e^+e^- annihilation into hadrons (hyperon pairs) is described in terms of the EMFFs. It is known that FFs are analytic functions and in the timelike region of the e^+e^- annihilation process for every value of the square of the transferred momentum q^2 , which is positive and corresponds to the square of the center-of-mass energy $q^2 = s > 0$. Therefore, FFs are introduced to take into account the non point-like structure of hadrons, because they play a fundamental role in understanding the

hadron dynamics.

In the formation of a nucleon-antinucleon pair ($\bar{N}N$) in the e^+e^- annihilation process in the Born approximation with a distorted wave, the effective EMFFs of a proton and a neutron in the timelike region were studied in [54].

Within the framework of the effective optical potential method [55], which describes well the $N\bar{N}$ scattering phases, the EMFFs G_E and G_M for protons and neutrons in the $p\bar{p}$ and $n\bar{n}$ production at the e^+e^- annihilation process near the threshold were used.

We want to emphasize that in [56, 57] it was suggested that by measuring the cross sections of hadron pair production in e^+e^- collisions for time-like regions, $q^2 > 0$, the electromagnetic form factors of hadrons can be studied.

In several experimental papers [58–65], at large q^2 [66, 67] there is an EMFF in the timelike region, which is consistent with the simple quark counting rules and the prediction of perturbative quantum chromodynamics (pQCD).

The study of strong and hadronic decays of $\psi(3770)$ in this energy region [68] provides knowledge about the structure of perturbative and non-perturbative strong interactions.

It is to be noted that already for several years BESIII Collaborations have been collecting the largest data sample at 3.773 GeV for e^+e^- collisions.

It is known that states at electron-positron colliders are produced from charmonium states with $J^{PC} = 1^{--}$ such as J/ψ , $\psi(3770)$, $\psi(4040)$, $\psi(4160)$, $Y(4230)$, $Y(4360)$, $\psi(4415)$, $Y(4660)$, and others as a result of the process of e^+e^- annihilation.

Therefore, to study the XYZ states, i.e., around the resonances $\psi(3770)$, $\psi(4040)$, $\psi(4160)$, $Y(4230)$, $Y(4360)$, $\psi(4415)$, $Y(4660)$ BESIII collected the largest data sample in the interval corresponding to the integrated luminosity from $5 fb^{-1}$ to $30 fb^{-1}$ in the energy range from 2.3864 to 4.95 GeV [69–74].

We would like to note that the decay process into light hadrons in these charmonium states occurs either via the one-photon process ($e^+e^- \rightarrow \psi \rightarrow \gamma^* \rightarrow hadrons$) or the three-gluon process ($e^+e^- \rightarrow \psi \rightarrow ggg \rightarrow hadrons$).

In fact, according to the Okubo-Zweig-Iizuka (OZI) rule, the lowest state of charmonium $\psi(3770)$, which lies 1^{--} above the $D\bar{D}$ threshold, will therefore predominantly decay to $D\bar{D}$ final states [48, 75, 76]. Studying the production of $\psi(3770)$ in e^+e^- annihilation and its subsequent decay into two hadrons in terms of the amplitudes of the quark distribution in hadron pairs and the conservation of the total hadron helicity is one of the ways to test the

QCD prediction.

We need to note that in the theory of hadron physics, the resonance of $\psi(3770)$ [77] at 3.770 GeV, due to the richness of $c\bar{c}$ states, turned out to be the only observed structure that exceeds the threshold for the production of an open charm pair of $D\bar{D}$ and, therefore, the exploration of such a resonance as $\psi(3770)$ is of great interest, which is one of those important structures in the hadron cross section.

Based on this, we note that the resonance of $\psi(3770)$ will almost completely decay into pure $D\bar{D}$ [48], and with an increase in the probability of the process due to a resonance such as J/ψ (or ψ) [78] the production of a baryon-antibaryon pair in the baryon sector at the e^+e^- collider can be verified by fundamental symmetries.

Note that the BESIII detector operating at the BEPCII collider in the energy range from 2.3864 to 4.95 GeV for different integrated luminosities has so far conducted high-precision studies of a possible threshold increase in the processes $e^+e^- \rightarrow \Sigma^\pm\bar{\Sigma}^\mp$ [73, 79], $\Xi^-\bar{\Xi}^+$ [70, 72], $\Sigma^0\bar{\Sigma}^0$ [71] and $\Xi^0\bar{\Xi}^0$ [74] and also showed that the cross section does not disappear near the threshold.

It should be noted that for measuring the near-threshold pair generation of hyperon production in the $e^+e^- \rightarrow \Xi^0\bar{\Xi}^0$ process, which was measured in the BESIII experiment [74], one can understand that the threshold effect obtained in this way will be useful.

It is worth noting that the process $e^+e^- \rightarrow \Xi^0\bar{\Xi}^0$ was studied both experimentally and also theoretically [80–85], and indeed, several experiments are of great importance for the development of high-energy particle physics. We should like to note that the aim of the present work is to explore the characteristics of the production of $\Xi^0\bar{\Xi}^0$ in the reaction $e^+e^- \rightarrow \Xi^0\bar{\Xi}^0$ including, in addition to the one-photon exchange, also the exchange of several states of charmonium (-like) $\psi(3770)$, $\psi(4040)$, $\psi(4160)$, $Y(4230)$, $Y(4360)$, $\psi(4415)$, $\psi(4660)$.

Considering the above, we can assume that experiments at current and future colliders are expected to provide an enormous amount of data and greatly increase our sensitivity to new physics if equally accurate predictions of the Standard Model are available.

II. THE PROCESS $e^+e^- \rightarrow \Xi^0\bar{\Xi}^0$ IN BORN APPROXIMATION

In the present section, we consider the $\Xi^0\bar{\Xi}^0$ production at the electron-positron annihilation reactions. The kinematics for the annihilation reaction is best described in the

center-of-mass (c.m.) system. This process is presented in the following form:

$$e^+(p_+) + e^-(p_-) \rightarrow \Xi^0(q_1) + \bar{\Xi}^0(q_2), \quad (1)$$

where p_+ and p_- are the momenta of the initial state positron and electron, and q_1 and q_2 are the momenta of the final state Ξ^0 and $\bar{\Xi}^0$ hyperons, respectively.

According to the process (1), we can define the Mandelstam invariants as follows:

$$\begin{aligned} s &= (p_+ + p_-)^2 = (q_1 + q_2)^2; \\ t &= (p_+ - q_1)^2 = (p_- - q_2)^2; \\ u &= (p_+ - q_2)^2 = (p_- - q_1)^2. \end{aligned} \quad (2)$$

Using the law of conservation of momentum, the sum of the Mandelstam variables satisfies the following expression:

$$s + t + u = 2m_e^2 + 2M_{\Xi}^2. \quad (3)$$

In this formula, m_e is the mass of the electron and M_{Ξ} is the Ξ^0 hyperon mass. When performing the calculation, we neglect the mass of the electron, m_e .

In the center-of-mass frame, the four-momenta of the electron (and positron) in the initial state and hyperons (Ξ^0) in the final state can be written as

$$\begin{aligned} p_- &= \frac{\sqrt{s}}{2}(1, 0, 0, 1), \quad p_+ = \frac{\sqrt{s}}{2}(1, 0, 0, -1), \\ q_1 &= \frac{\sqrt{s}}{2}(1, \beta \sin \theta_{\Xi}, 0, \beta \cos \theta_{\Xi}), \quad q_2 = \frac{\sqrt{s}}{2}(1, -\beta \sin \theta_{\Xi}, 0, -\beta \cos \theta_{\Xi}). \end{aligned}$$

In general, in the Born approximation, the differential cross section for the annihilation reaction (1) in the center-of-mass system, can be written in the following form:

$$d\sigma = \frac{1}{8s} \sum_{\text{spins}} |M|^2 d\Phi_2. \quad (4)$$

Here the sum is performed over all spin states in the matrix element squared. In the center-of-mass frame element of phase space of the final particles, $d\Phi_2$ is in the following form:

$$\begin{aligned} d\Phi_2 &= (2\pi)^4 \delta(p_+ + p_- - q_1 - q_2) \frac{d\mathbf{q}_1}{(2\pi)^3 2E_1} \frac{d\mathbf{q}_2}{(2\pi)^3 2E_2} = \\ &= \frac{|\mathbf{q}|}{16\pi^2 \sqrt{s}} d\Omega_{\Xi} = \frac{\beta}{16\pi} d\cos \theta_{\Xi}, \end{aligned} \quad (5)$$

where $d\Omega = d\phi_{\Xi}d(\cos\theta_{\Xi})$ is the solid angle of particle Ξ . ϕ_{Ξ} is the azimuthal angle and θ_{Ξ} is the polar angle of the final Σ -hyperon in the e^+e^- center-of-mass reference frame, i.e., θ_{Ξ} is the angle between 3-momenta of the directions of the initial electron \mathbf{p}_- and the final Ξ -hyperon \mathbf{q}_1 (Fig. 1). Here the modulus of 3-momenta of the final Ξ^0 -hyperon (or $\bar{\Xi}^0$ -hyperon) can be determined by the δ -function in the phase space, i.e.,

$$|\mathbf{q}| \equiv |\mathbf{q}_1| = |\mathbf{q}_2| = \frac{\sqrt{s}}{2} \sqrt{1 - \frac{4M_{\Xi}^2}{s}} = \frac{\sqrt{s}}{2} \beta, \quad (6)$$

where $\beta = \sqrt{1 - \frac{4M_{\Xi}^2}{s}}$ is the velocity of the final hyperon in the e^+e^- c.m. system, s is the e^+e^- total c.m. energy squared, and M_{Ξ} is the mass of the Ξ^0 -hyperon.

Figure 2(a) shows the Feynman diagrams in the Born approximation for the formation of a hyperon pair $\Xi^0\bar{\Xi}^0$, where e^+e^- annihilates (1) into a virtual photon.

It is known that processes such as (1), which are shown in Fig. 2(a), are described by a purely electrodynamic diagram. In the Born approximation, the amplitude for the process $\mathcal{M}_B(e^+e^- \rightarrow \Xi^0\bar{\Xi}^0)$ (1) can be written as:

$$\mathcal{M}_B = \frac{1}{s} J_{\mu}^{e\bar{e} \rightarrow \gamma}(q) J_{\gamma \rightarrow \Xi^0\bar{\Xi}^0}^{\mu}(q) \quad (7)$$

where $s = q^2 = (p_+ + p_-)^2 = (q_1 + q_2)^2$ represents the invariant mass squared of the e^+e^- system. The functions $J_{\mu}^{e\bar{e}(q) \rightarrow \gamma}$ and $J_{\gamma \rightarrow \Xi^0\bar{\Xi}^0}^{\mu}(q)$ from (7) represent the lepton and hyperon electromagnetic currents, they can be written as follows:

$$J_{\mu}^{e\bar{e} \rightarrow \gamma}(q) = -e[\bar{v}(p_+)\gamma_{\mu}u(p_-)], \quad (8)$$

$$J_{\gamma \rightarrow \Xi^0\bar{\Xi}^0}^{\mu}(q) = e[\bar{u}(q_1)\Gamma_{\mu}(q)v(q_2)], \quad (9)$$

where e is the modulus electron charge $e = \sqrt{4\pi\alpha}$ and $\alpha \approx 1/137$ is the quantum electrodynamics (QED) fine structure constant [77].

To describe the structure of hyperons (baryons) and the exploration of this process in detail, we introduce form factors. Using the Pauli form factors F_1 and F_2 for this annihilation process, which is shown in Fig. 2(a), we can write the current as $\gamma\Xi^0\bar{\Xi}^0$ ($\gamma B\bar{B}$). In general, the vertex function $\Gamma_{\mu}(q)$ describing a photon with Ξ hyperons [Fig. 2(a)] is represented in terms of the electromagnetic hyperon form factor:

$$\Gamma_{\mu}(q) = F_1(q^2)\gamma_{\mu} - \frac{F_2(q^2)}{4M_{\Xi}}(\gamma_{\mu}\hat{q} - \hat{q}\gamma_{\mu}), \quad (10)$$

where we use the notation: $\hat{q} = q_\nu \gamma^\nu$, M_Ξ and q are the hyperon mass and transferred momentum in the center-of-mass of the system, respectively. In (10), the form factors of the Ξ -hyperons $F_1(q^2)$ and $F_2(q^2)$ are usually normalized as follows: $F_1(0) = 0$ and $F_2(0) = \mu_\Xi$, where μ_Ξ is the anomalous magnetic moment of the Ξ -hyperon.

However, a recent analysis [86] has shown that the point-like behavior of the hadron near the threshold is not so unique and the nontrivial structure of the baryon begins to manifest itself already at relatively small q^2 . In [87], it was suggested that in the energy range we are considering, i.e., $\sqrt{s} \sim 3 - 5 \text{ GeV}$, the approximation of point-like hadrons is not valid. Therefore, in the present work, we use the effective form factor $G(s)$. Besides, without taking into account the form factor, it will be impossible to compare the Born cross section with the experimental data.

It should be noted that in the time-like region there is little statistics and, therefore, the experimental data contain large errors. At the moment the experiment does not allow us to highlight the electric G_E and magnetic G_M form factors. Considering this, we use the assumption that $|G_E| = |G_M|$, i.e., $F_2(q^2) = 0$. We want to choose the form factor F_1 such that it has a pQCD-inspired form [66, 88] and also takes into account the running of the QCD coupling constant α_s .

We can square the matrix element in (7) and further calculate the trace techniques and after that, take into account the form factor $F_1(q^2) = G(q^2)$. Then for the square of the amplitude we obtain the expression in the following form:

$$\sum_{spins} |\mathcal{M}_B|^2 = 64\pi^2\alpha^2 |G(s)|^2 (2 - \beta^2 \sin^2 \theta_\Xi). \quad (11)$$

Let us put the formulae for the square of the matrix element (11) and for the phase volume (5) in formula (4). Then, in general, for the differential cross section we obtain an expression in the following form:

$$\frac{d\sigma_B(s)}{d\cos\theta_\Sigma} = \frac{\pi\alpha^2\beta}{2s} |G(s)|^2 (2 - \beta^2 \sin^2 \theta_\Xi). \quad (12)$$

To obtain an expression for the total cross section, we must perform integrations in (12) over all possible scattering angles $d\cos\theta_\Xi = \sin\theta_\Xi d\theta_\Xi$.

The limits of integration over the angles θ_Ξ are defined in this interval $[0 \leq \theta_\Xi \leq \pi]$.

Thus, after performing the integration over the angles θ_Ξ in formula (12), we obtain an

expression for the total cross section in the Born approximation in the following form:

$$\sigma_B(s) = \frac{2\pi\alpha^2}{3s}\beta(3 - \beta^2)|G(s)|^2. \quad (13)$$

Here we use the effective form factor $G(s)$ applied in pQCD [66, 88], which takes into account the current QCD coupling constant α_s

$$G(s) = \frac{C}{s^2 \log^2(s/\Lambda_{QCD}^2)}, \quad (14)$$

where the constant C is a free parameter that is fitted based on experimental data and the quantity Λ_{QCD} is the QCD scale parameter. Note that in this process the constant C is fitted for the production of a hyperon pair $\Xi^0\bar{\Xi}^0$ according to specific experimental data of the BESIII in the energy range of the corresponding experiment.

In our case, for the $\Xi^0\bar{\Xi}^0$ pair production, we fix the constant C using the whole BESIII measurement range [74], and the obtained results on the dependence of the total cross section on the center-mass-energy \sqrt{s} are shown in Fig. 3. In the Born cross section from (13) if we accept for the quantity $\Lambda_{QCD} = 300$ MeV, then for the parameter C after fitting respect to these data we gives us the following parameter:

$$C = (64.68 \pm 1.3) \text{ GeV}^4. \quad (15)$$

These values of C and Λ_{QCD} are further used in our numerical calculations for the electromagnetic form factor Ξ -hyperon (14). It should be noted that this expression for the form factor $G(s)$ (14) with the parameter C from (15) works in the region of relatively large transferred momentum q^2 .

The threshold near the Coulomb-like amplification factor with many subtle features plays an important role [52, 89] or it manifests the wave nature of the hyperon stabilization after its exit from the vacuum [86]. Therefore, it can not be applied to work near the threshold.

III. THE QUARKONIUM $\psi(3770)$ INTERMEDIATE STATE

In the present paper, for the $\Xi^0\bar{\Xi}^0$ production in the e^+e^- annihilation process, the main task is to describe the excitation effect of the charmonium resonance $\psi(3770)$. It can be seen from Fig. 3 that the total cross section in the Born approximation of the process (1), which includes only the electromagnetic mechanism (13), in the vicinity of the charmonium

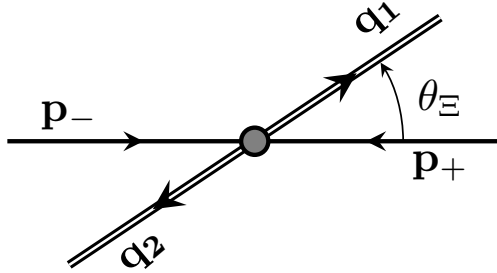


Figure 1: The definition of the scattering angle θ_{Ξ} from (5) in the center-of-mass reference system.

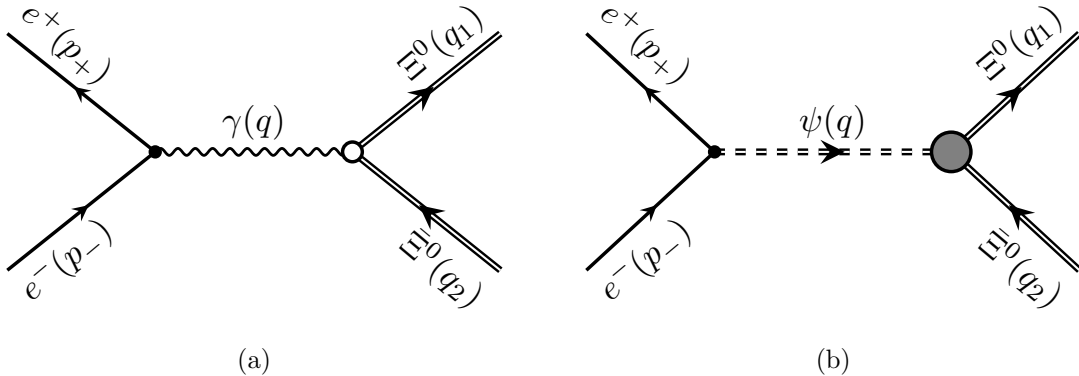


Figure 2: The Feynman diagrams for the $\Xi^0\bar{\Xi}^0$ hyperon pair production in the e^+e^- annihilation process corresponding to the one-photon exchange (a) and the intermediate state $\psi(3770)$ charmonium (b).

resonance $\psi(3770)$ cannot describe the subtle behavior. For a detailed study of the process (1) we need to take into account in this region an additional contribution to the amplitude, which arises from the diagram with $\psi(3770)$ in the intermediate state (Fig. 2(b)) and is enhanced by the Breit-Wigner propagator. Next, we develop a model (based on our previous calculations [90–94]) that fully explores the basic mechanism for this process (1). Therefore, in the region of excitation of the charmonium resonance $\psi(3770)$ [$I^G(J^{PC}) = 0^-(1^{--})$] in the intermediate state we must compute the contribution of an additional mechanism. The total amplitude of the process $\mathcal{M}_B(e^+e^- \rightarrow \Xi^0\bar{\Xi}^0)$ (1) then becomes the sum of two matrix elements:

$$\mathcal{M} = \mathcal{M}_B + \mathcal{M}_\psi, \quad (16)$$

where \mathcal{M}_B is the amplitude in the Born approximation (Fig. 2(a)) from (7) for the process (1) and \mathcal{M}_ψ is the amplitude that accounts for the mechanism with charmonium $\psi(3770)$

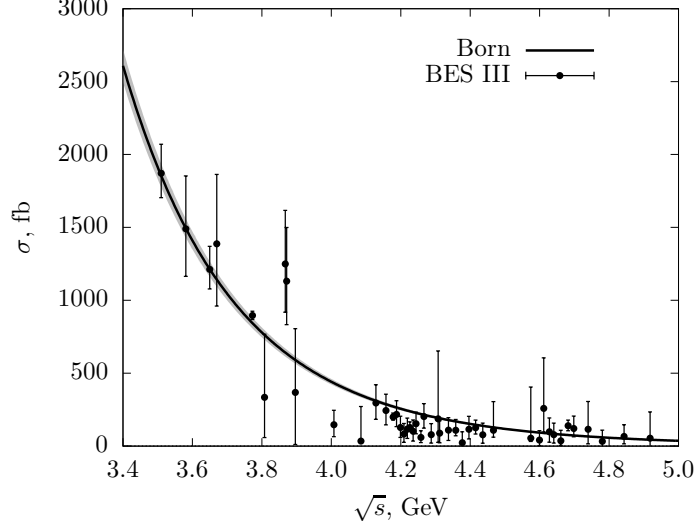


Figure 3: Total cross section distributions of the process $e^+e^- \rightarrow \Xi^0\bar{\Xi}^0$ as a function of the center-of-mass energy \sqrt{s} . The Experimental data are from BESIII Collaboration [74]. The theoretical curve for the total cross section in the Born approximation (13) is indicated by black lines. Due to errors in fitting of the form factor constant (15), curve errors occur.

for the intermediate state with the enhanced Breit-Wigner factor [Fig. 2(b)],

$$M_\psi = \frac{1}{s - M_\psi^2 + iM_\psi\Gamma_\psi} J_\mu^{e\bar{e}\rightarrow\psi}(q) \left(g^{\mu\nu} - \frac{q^\mu q^\nu}{M_\psi^2} \right) J_\nu^{\psi\rightarrow\Xi^0\bar{\Xi}^0}(q), \quad (17)$$

where M_ψ is the mass of the $\psi(3770)$, $M_\psi = 3773.7$ MeV, and the $\Gamma_\psi = 27.2$ MeV [77] is the total decay width of the $\psi(3770)$ resonance. The current $J_\mu^{e\bar{e}\rightarrow\psi}(q)$ describes the transition of the electron-positron pair to the resonance $\psi(3770)$ and the current $J_\nu^{\psi\rightarrow\Xi^0\bar{\Xi}^0}(q)$ describes the transition of the resonance $\psi(3770)$ to the hyperon-antihyperon pair, respectively. We know that the currents in (17) must be conserved, that is, $q^\mu J_\mu^{e\bar{e}\rightarrow\psi}(q) = q^\mu J_\mu^{\psi\rightarrow\Xi^0\bar{\Xi}^0}(q) = 0$. Based on the work [90], we assume that the vector current $J_\mu^{e\bar{e}\rightarrow\psi}(q)$ has also the same structure as in the case of the photon, that is, $J_\mu^{e\bar{e}\rightarrow\gamma}$, then the vector current, according to (8), can be written in this form:

$$J_\mu^{e\bar{e}\rightarrow\psi}(q) = g_e [\bar{v}(p_+) \gamma_\mu u(p_-)], \quad (18)$$

where the constant $g_e = F_1^{\Xi^0\bar{\Xi}^0}(M_\psi^2)$ is equal to the value of the form factor $F_1^{\psi\rightarrow\Xi^0\bar{\Xi}^0}(M_\psi^2)$ for the vertex $\psi \rightarrow \Xi^0\bar{\Xi}^0$ on the $\psi(3770)$ mass shell [here we assume that in the case of the Born approximation $F_2^{\psi\rightarrow\Xi^0\bar{\Xi}^0}(M_\psi^2) = 0$]. Note that from [77] we know the total decay width

$\psi \rightarrow e^+e^-$ which is $\Gamma_{\psi \rightarrow e^+e^-} = 261 \text{ eV}$. Knowing this, we can compute the constant g_e ,

$$g_e = \sqrt{\frac{12\pi\Gamma_{\psi \rightarrow e^+e^-}}{M_\psi}} = 1.6 \cdot 10^{-3}. \quad (19)$$

Based on the work of [95], we can neglect the possible imaginary part of the vertex $e\bar{e} \rightarrow \psi$, because in this work it was shown that the imaginary part of the vertex is less than 10 % of the real part. Considering this, we do not include this source of error when calculating the statistical uncertainty of our final results.

Using the total matrix element of (16) and taking into account the contribution of charm to the intermediate state and, accordingly, the general formula for the total cross section (4) for the total cross section, we obtain the expression in the following form:

$$\begin{aligned} \sigma &\sim |\mathcal{M}|^2 = ||\mathcal{M}_B| + e^{i\phi}|\mathcal{M}_\psi||^2 = \\ &= |\mathcal{M}_B|^2 + 2 \cos \phi |\mathcal{M}_B| \cdot |\mathcal{M}_\psi| + |\mathcal{M}_\psi|^2 \sim \sigma_B + \sigma_{int} + \sigma_\psi, \end{aligned} \quad (20)$$

where ϕ is the relative phase between the Born amplitude \mathcal{M}_B and the additional contribution \mathcal{M}_ψ of the intermediate state $\psi(3770)$ of the charmonium.

Thus, we have to compute the contribution of the charmonium σ_ψ to the cross section and the interference contribution of the Born amplitude in σ_{int} with the charmonium amplitude to σ_ψ . Knowing the Born section σ_B from (13) and the interference contribution of σ_{int} with a phase ϕ , using (20) we can calculate the full total cross section including both contributions, and after that we can evaluate σ_ψ as follows:

$$\sigma_\psi = \left(\frac{\sigma_{int}}{2 \cos \phi \sqrt{\sigma_B}} \right)^2. \quad (21)$$

Based on the general formula (4), we can calculate the interference of the Born contribution \mathcal{M}_B with the contribution of the intermediate state $\psi(3770)$ charmonium \mathcal{M}_ψ , which is represented in the following standard form:

$$d\sigma_{int} = \frac{1}{8s} \sum_{\text{spins}} 2 \text{Re}[\mathcal{M}_B^\dagger \mathcal{M}_\psi] d\Phi_2, \quad (22)$$

Here our goal is that we want to obtain the contribution to the total cross section.

Therefore, after performing integration over the phase space of the final particles in (22), we get the following formulas for the contribution to the total cross section:

$$\sigma_{int}(s) = \frac{1}{4s^2} \text{Re} \left\{ \frac{\sum_s (J_\mu^{e\bar{e} \rightarrow \gamma})^* J_\nu^{e\bar{e} \rightarrow \psi}}{s - M_\psi^2 + iM_\psi \Gamma_\psi} \cdot \sum_{s'} \int d\Phi_2 (J_{\gamma \rightarrow \Xi^0 \Xi^0}^\mu)^* J_{\psi \rightarrow \Xi^0 \Xi^0}^\nu \right\}, \quad (23)$$

where \sum_s and $\sum_{s'}$ are the summation over the spin states of the initial and final particles, respectively. Here after using the procedure of the invariant integration method over the total volume of the final phase, for the second term in (23) we get the expression as follows:

$$\sum_{s'} \int d\Phi_2 (J_{\gamma \rightarrow \Xi^0 \bar{\Xi}^0}^\mu)^* J_{\psi \rightarrow \Xi^0 \bar{\Xi}^0}^\nu = \frac{1}{3} \left(g^{\mu\nu} - \frac{q^\mu q^\nu}{q^2} \right) \sum_{s'} \int d\Phi_2 \left(J_{\gamma \rightarrow \Xi^0 \bar{\Xi}^0}^\alpha \right)^* J_\alpha^{\psi \rightarrow \Xi^0 \bar{\Xi}^0}. \quad (24)$$

In these cases, we use explicit expressions for lepton currents $J_\mu^{e\bar{e} \rightarrow \gamma}$ from (7) and $J_\nu^{e\bar{e} \rightarrow \psi}$ from (18) and take into account the law of conservation of currents; then, based on this, we can compute

$$\begin{aligned} \sum_s (J_\mu^{e\bar{e} \rightarrow \gamma})^* J_{e\bar{e} \rightarrow \psi}^\mu &= -eg_e \sum_s [\bar{u}(p_-) \gamma_\mu v(p_+)] [\bar{v}(p_+) \gamma^\mu u(p_-)] \approx \\ &\approx -eg_e \text{Tr}[\hat{p}_- \gamma_\mu \hat{p}_+ \gamma^\mu] \approx 4e g_e s. \end{aligned} \quad (25)$$

Using the expression for the two-particle phase volume of the final particles from (5), the invariant integration method from (24) and the result from (25), substituting all this into formula (23), for the interference contribution to the total cross section we then get the following expression:

$$\sigma_{int}(s) = \frac{eg_e \beta}{48\pi s} \text{Re} \left\{ \frac{1}{s - M_\psi^2 + iM_\psi \Gamma_\psi} \int_{-1}^1 d \cos \theta_{\Xi^0} \sum_{s'} (J_{\gamma \rightarrow \Xi^0 \bar{\Xi}^0}^\alpha)^* J_\alpha^{\psi \rightarrow \Xi^0 \bar{\Xi}^0} \right\}. \quad (26)$$

The subintegral expression in (26) can be represented in a separate form, since it contains the dynamics of the transformation of charmonium into a pair, $\Xi^0 \bar{\Xi}^0$, that is

$$S_i(s) = \frac{eg_e \beta}{48\pi s} \int_{-1}^1 d \cos \theta_{\Xi^0} \sum_{s'} (J_{\gamma \rightarrow \Xi^0 \bar{\Xi}^0}^\alpha)^* J_\alpha^{\psi \rightarrow \Xi^0 \bar{\Xi}^0}. \quad (27)$$

Thus, if we take into account formulae (27) in (26), then for the interference contribution to the total cross section we can represent $\sigma_{int}(s)$ in the form

$$\sigma_{int}(s) = \text{Re} \left(\frac{S_i(s)}{s - M_\psi^2 + iM_\psi \Gamma_\psi} \right), \quad (28)$$

Different mechanisms of this transformation in formulae (27) and (28) are denoted by i in the subscript. We know that the mass of $\psi(3770)$ exceeds the threshold for the production of a $D\bar{D}$ pair; thus, it is natural to expect the D -meson loop to be the main mechanism in this reaction. Considering this, in Fig. 4 we present a Feynman diagram, which describes quite possibly the usual OZI-permitted mechanism via the D -meson loop.

However, according to this mechanism, the threshold excess is very small, i.e., the mass $\psi(3770)$ slightly exceeds the threshold of pair production of D -mesons (it can be seen that $(M_\psi - 2M_D)/M_\psi \approx 1\%$). For this, we suggest considering the OZI breaking mechanism due to the charmonium three-gluon annihilation into the $\Xi^0\bar{\Xi}^0$ pair (see Fig. 5), which gives the dominant contribution.

Now, given the interference contribution (28) with the total relative phase between the Born amplitude \mathcal{M}_B and the charmonium contribution \mathcal{M}_ψ , we can restore the total cross section. It is worth noting that in this case, we will use the procedure described in [91] [equations (15) and (16)].

IV. THE D -MESON LOOP MECHANISM

In this process, we will also follow our previous calculations [90–94] with only one systematic modification which is necessary to describe the final state of the $\Xi^0\bar{\Xi}^0$ pair. Thus, in this section, we consider the contribution of the intermediate charmonium with the transition to the final state of the $\Xi^0\bar{\Xi}^0$ hyperon pair via the D -meson loop. In Fig. 4, we can illustrate the Feynman diagram for the production of $\Xi^0\bar{\Xi}^0$ via the D -meson loop mechanism. To calculate $\sigma_{int}(s)$ from (28), we first need to calculate the contribution of the D -meson loop, that is, the quantity S_D from (27). Thus, according to Feynman's rules, we can write the amplitude \mathcal{M}_D (according to Fig. 4) and from this amplitude we can extract the value S_D . The amplitude \mathcal{M}_D has the following form:

$$\mathcal{M}_D = \frac{g_e}{16\pi^2} \frac{[\bar{v}(p_+)\gamma_\mu u(p_-)]}{q^2 - M_\psi^2 + iM_\psi \Gamma_\psi} \cdot \int \frac{dk}{i\pi^2} \frac{[\bar{u}(q_+)\gamma_5(\hat{k} + M_\Sigma)\gamma_5 v(q_2)](2k + q_2 - q_1)^\mu}{(k^2 - M_\Sigma^2)((k - q_1)^2 - M_D^2)((k + q_2)^2 - M_D^2)} \times \\ \times G_{\psi D\bar{D}}(q^2, (k + q_2)^2, (k - q_1)^2) G_{\Sigma D\Xi}(k^2, (k - q_1)^2) G_{\Sigma D\bar{\Xi}}(k^2, (k + q_2)^2), \quad (29)$$

where M_ψ is the mass of the $\psi(3770)$ -charmonium, M_D is the mass of the D -meson, and M_Σ is the mass of the Σ -hyperon, respectively. Thus, for the vertex $\psi D\bar{D}$, we use the form factor dependence in the following form:

$$G_{\psi D\bar{D}}(s, M_D^2, M_D^2) = g_{\psi D\bar{D}} \frac{M_\psi^2}{s} \frac{\log(M_\psi^2/\Lambda_D^2)}{\log(s/\Lambda_D^2)}, \quad (30)$$

where the scale Λ_D is fixed on the characteristic value of the reaction $\Lambda_D = 2M_D$. If we compare expression (29) with the general form of the amplitude from (17), for the current

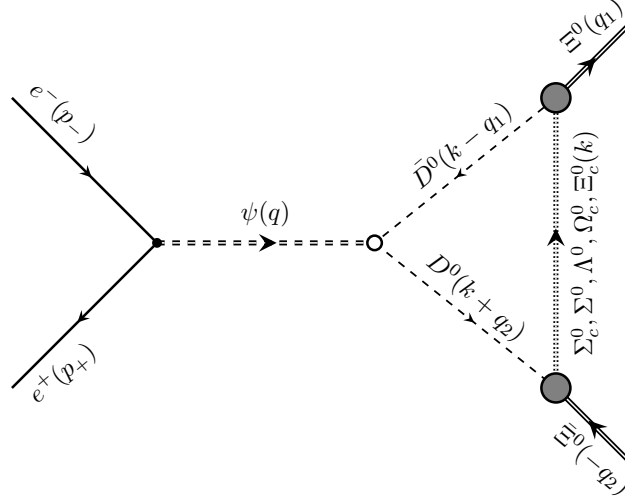


Figure 4: The Feynman diagram for the $\Xi^0\bar{\Xi}^0$ hyperon pair production in charmonium decays through the D -meson loop mechanism in the e^+e^- annihilation process at the one-loop level.

$J_\nu^{\psi \rightarrow \Xi^0\bar{\Xi}^0}(q)$ we have an expression in the following form:

$$J_\mu^{\psi \rightarrow \Xi^0\bar{\Xi}^0}(q) = \frac{1}{16\pi^2} \int \frac{dk}{i\pi^2} \frac{[\bar{u}(q_+) \gamma_5 (\hat{k} + M_\Sigma) \gamma_5 v(q_2)] (2k + q_2 - q_1)^\mu}{(k^2 - M_\Sigma^2)((k - q_1)^2 - M_D^2)((k + q_2)^2 - M_D^2)} \times \\ \times G_{\psi D\bar{D}}(q^2, (k + q_2)^2, (k - q_1)^2) G_{\Sigma D\Xi}(k^2, (k - q_1)^2) G_{\Sigma D\Xi}(k^2, (k + q_2)^2), \quad (31)$$

and it is included in (27). It is worth noting that the D -meson loop mechanism (Fig. 4) with the Born amplitude contributes to the interference of a charmonium state (see (27)).

In this case, for S_D (27) we get an expression in the following form:

$$S_D(s) = \frac{\alpha g_e \beta G(s)}{48\pi^2 s} \int \frac{dk}{i\pi^2} \frac{Tr D(s, k^2)}{(k^2 - M_\Sigma^2)((k - q_1)^2 - M_D^2)((k + q_2)^2 - M_D^2)} \times \\ \times G_{\psi D\bar{D}}(q^2, (k + q_2)^2, (k - q_1)^2) G_{\Sigma D\Xi}(k^2, (k - q_1)^2) G_{\Sigma D\Xi}(k^2, (k + q_2)^2 = \\ \alpha_D(s) Z_D(s). \quad (32)$$

From this formula, the quantities $\alpha_D(s)$ and $Z_D(s)$ can be written separately, which have the following forms:

$$\alpha_D(s) = \frac{\alpha g_e \beta G(s)}{48\pi^2}, \\ Z_D(s) = \frac{1}{s} \int \frac{dk}{i\pi^2} \frac{Tr D(s, k^2)}{(k^2 - M_\Sigma^2)((k - q_1)^2 - M_D^2)((k + q_2)^2 - M_D^2)} \times \\ \times G_{\psi D\bar{D}}(q^2, (k + q_2)^2, (k - q_1)^2) G_{\Sigma D\Xi}(k^2, (k - q_1)^2) G_{\Sigma D\Xi}(k^2, (k + q_2)^2). \quad (33)$$

where $TrD(s, k^2)$ is the trace of the γ -matrix along the baryon line, which can be written in the following form:

$$\begin{aligned} TrD(s, k^2) &= Tr[(\hat{q}_+ + M_\Xi)\gamma_5(\hat{k} + M_\Sigma)\gamma_5(\hat{q}_2 - M_\Xi)(\hat{k} - M_\Xi)] = \\ &= 2((k^2)^2 + k^2(s - 2(M_D^2 + M_\Xi M_\Sigma)) - sM_\Xi M_\Sigma + c_D), \end{aligned} \quad (34)$$

where c_D has the following form:

$$c_D = M_D^4 + 2M_\Xi M_\Sigma M_D^2 + 2M_\Sigma M_\Xi^3 - M_\Xi^4. \quad (35)$$

It should be noted that in formula (32), the quantities $G_{\psi D\bar{D}}$ and $G_{\Xi D\Sigma}$ for the vertices $\psi \rightarrow D\bar{D}$ and $D \rightarrow \Xi\Sigma$ are the form factors [62, 71, 73, 74, 96].

Now we need to compute the quantity of $Z_D(s)$ from (33). For this aim we use the Cutkosky cutting rules [97] for the D -meson propagators in (33) to equivalently replace them through the delta function:

$$\begin{aligned} \frac{1}{(k - q_1)^2 - M_D^2} \frac{1}{(k + q_2)^2 - M_D^2} &\longrightarrow (-2\pi i)^2 \delta((k - q_1)^2 - M_D^2) \theta(-(k - q_1)_0) \cdot \\ &\cdot \delta((k + q_2)^2 - M_D^2) \theta((k + q_2)_0). \end{aligned} \quad (36)$$

Then we use these delta functions (36) and get the imaginary part of this quantity from $Z_D(s)$,

$$\begin{aligned} 2i \text{Im } Z_D(s) &= \frac{(-2\pi i)^2}{s} \int \frac{dk}{i\pi^2} \frac{TrD(s, k^2)}{k^2 - M_\Xi^2} G_{\psi D\bar{D}}(s, (k + q_2)^2, (k - q_1)^2) \times \\ &\times G_{\Sigma D\Xi}(k^2, (k - q_1)^2) G_{\Sigma D\Xi}(k^2, (k + q_2)^2) \delta((k + q_2)^2 - M_D^2) \delta((k - q_1)^2 - M_D^2) \times \\ &\times \theta((k + q_2)_0) \theta(-(k - q_1)_0). \end{aligned} \quad (37)$$

We note that by replacing these two delta functions in (37) and implementing cyclic integrations to significantly simplify the evaluation of $\text{Im } Z_D$, we obtain the final expression for the imaginary part of this value in the following form:

$$\begin{aligned} \text{Im } Z_D(s) &= -\frac{2\pi}{s^{3/2}} G_{\psi D\bar{D}}(s, M_D^2, M_D^2) \int_{C_k^{(1)}} \frac{dC_k}{\sqrt{D_1}} \sum_{i=1,2} \frac{k_{(i)}^2}{k_{(i)}^2 + M_\Xi^2} \times \\ &\times TrD(s, -k_{(i)}^2) G_{\Sigma D\Xi}^2(-k_{(i)}^2, M_D^2). \end{aligned} \quad (38)$$

Here $s > 4M_D^2$, whereas integration over the cosine of the polar angle $C_k = \cos \theta_k$ is calculated numerically. To do this, we can define the values of $k_{(i)}$, D_1 , and $C_k^{(1)}$ as

$$k_{(1,2)} = \frac{1}{2}(\sqrt{s} \beta C_k \pm \sqrt{D_1}), \quad D_1 = s \beta^2 C_k^2 - 4(M_D^2 - M_\Xi^2), \quad C_k^{(1,2)} = \pm \frac{2}{\beta} \sqrt{\frac{M_D^2 - M_\Xi^2}{s}}. \quad (39)$$

Now we must consider the explicit expression of the form factors to perform the calculations of $\text{Im } Z_D$ from (38). It should be noted that for the vertex $\psi \rightarrow D\bar{D}$ we only need the dependence on the charmonium virtuality $q^2 = s$. In this case, we assume that the legs of the D meson are on-mass-shell, and then using expression (38), we calculate the imaginary part of Z_D .

It should be noted that the details of the calculation of $Z_D(s)$ are in [90, 91]; however, in the present work we technically compute the imaginary part of this quantity and then, by applying the dispersion relation with one subtraction at $q^2 = 0$, we restore its real part. Also, it is worth noting that the subtraction constant here also vanishes, since the Ξ hyperon (which is the uss quark state) has no open charm and, therefore, at $q^2 = 0$ the vertex $\psi \rightarrow \Xi^0\bar{\Xi}^0$ is zero.

The normalizations of the function $G_{\psi D\bar{D}}(s, M_D^2, M_D^2)$ to the decay of the charmonium $\psi(3770)$ into the final state $D\bar{D}$ must be fixed. The decay width $\psi \rightarrow D\bar{D}$ is used to fix these functions,

$$g_{\psi D\bar{D}} \equiv G_{\psi D\bar{D}}(M_\psi^2, M_D^2, M_D^2). \quad (40)$$

To have a vertex $\psi \rightarrow D\bar{D}$ with the only dependence on charmonium virtuality $q^2 = s$, it is necessary to cut the diagram by D -meson propagators, since the D -meson legs are on the mass shell.

To determine the value of the constant $g_{\psi D\bar{D}}$, we need to know the decay widths of the charmonium $\psi \rightarrow D\bar{D}$. We can write the standard formula for calculating the total decay width in the following form:

$$\Gamma_{\psi D\bar{D}} = \frac{g_{\psi D\bar{D}}^2 M_\psi \beta_D^3}{48\pi}. \quad (41)$$

Now we can calculate the value of the constant $g_{\psi D\bar{D}}$. For this we use the experimental value of the decay width of the charmonium $\Gamma_{\psi D\bar{D}} = 25 \text{ MeV}$ [77] and then compute the constants $g_{\psi D\bar{D}}$, and accordingly obtain the following value:

$$g_{\psi D\bar{D}} = 4\sqrt{\frac{3\pi\Gamma_{\psi D\bar{D}}}{M_\psi\beta_D^3}} \approx 18.4, \quad (42)$$

where $\beta_D = \sqrt{1 - 4M_D^2/M_\psi^2}$ is the D -meson velocity in the $\psi \rightarrow D\bar{D}$ decay.

It should be noted that we need to consider the function $G_{\Sigma D\Xi}(k^2, p^2)$ from (33). We know that the only dependence left in the t -channel in the imaginary part of Z_D is the off-mass shell of the Ξ -baryon, since here $k^2 = -k_{(i)}^2 < 0$.

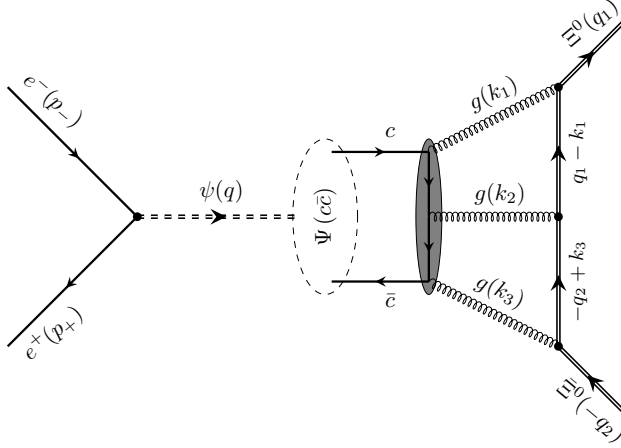


Figure 5: The Feynman diagram of the $\Xi^0\bar{\Xi}^0$ hyperon pair production in charmonium decays through the three-gluon mechanism in the e^+e^- annihilation process.

We would like to point out that in [90–92] we used the ΛDP -vertex based on the results of [98, 99]. In [93, 94], we used a constant for the $\Xi D\Sigma$ -vertex, which is based on the results of [99, 100]. However, in the present paper we use for the $\Sigma D\Xi$ -vertex another form of constant according to the results of [99, 100].

It is necessary to note that the $SU(4)$ symmetry leads us to the same result for the function $G_{\Sigma D\Xi}$,

$$G_{\Xi D\Sigma}(k^2, M_D^2) = \frac{f_D g_{\Sigma D\Xi}}{m_u + m_c}, \quad k^2 < 0, \quad (43)$$

where $f_D \approx 180$ MeV and

$$g_{\Sigma D\Xi} \approx g_{K\Sigma\Xi} = -7.02. \quad (44)$$

For the mass of u and c quarks, we apply the following values: $m_u \approx 280$ MeV and $m_c = 1.27$ GeV [77].

V. THE THREE-GLUON MECHANISM

In this section, we present how the intermediate charmonium contributes to the production of the $\Xi^0\bar{\Xi}^0$ pair through the three-gluon annihilation mechanism. Here we compute the quantity of S_{3g} from (27) to determine the contribution of S_{3g} to the cross section (28). The Feynman diagram for the production of a $\Xi^0\bar{\Xi}^0$ hyperon pair via the three-gluon mechanism in the e^+e^- annihilation is presented in Fig. 5. We would like to note that a reaction

similar to ours, i.e., the production of a pair of hadrons in the process of annihilation of e^+e^- through the three-gluon mechanism was considered in [90, 91]; it was revised and some typos and minor errors were corrected. In this work, we also apply this mechanism to the reaction $e^+e^- \rightarrow \Xi^0\bar{\Xi}^0$ via the three-gluon exchange.

Therefore, we present the final formulae for the contribution to the quantity of S_{3g} from (28) in the interference of the charmonium state with the Born amplitude [see (27)] according to the relevant Feynman diagram (Fig. 5), [which coincide with Eqs. (16) and (17) from [90]]:

$$S_{3g}(s) = \alpha_{3g}(s) Z_{3g}(s), \quad (45)$$

where

$$\alpha_{3g}(s) = \frac{\alpha \alpha_s^3}{2^3 3} g_e g_{col} \phi \beta G(s) G_\psi(s), \quad (46)$$

$$Z_{3g}(s) = \frac{4}{\pi^5 s} \int \frac{dk_1}{k_1^2} \frac{dk_2}{k_2^2} \frac{dk_3}{k_3^2} \frac{Tr3g \delta(q - k_1 - k_2 - k_3)}{((q_1 - k_1)^2 - M_\Xi^2)((q_2 - k_3)^2 - M_\Xi^2)}, \quad (47)$$

where g_{col} is the color factor, $g_{col}(1/4) = \langle \Sigma | d^{ijk} T^i T^j T^k | \Sigma \rangle = 15/2$. The $Tr3g$ is the product of traces over the Ξ -hyperon and c -quark lines,

$$Tr3g = \text{Tr}[\hat{Q}_{\alpha\beta\gamma}(\hat{k}_c + m_c)\gamma^\mu(\hat{k}_{\bar{c}} - m_c)] \cdot \text{Tr} \left[(\hat{q}_1 + M_\Xi)\gamma^\alpha(\hat{q}_1 - \hat{k}_1 + M_\Xi)\gamma^\beta \times \right. \\ \left. \times (-\hat{q}_2 + \hat{k}_3 + M_\Xi)\gamma^\gamma(\hat{q}_2 - M_\Xi)\gamma_\mu \right],$$

where

$$\hat{Q}_{\alpha\beta\gamma} = \frac{\gamma_\gamma(-\hat{k}_{\bar{c}} + \hat{k}_3 + m_c)\gamma_\beta(\hat{k}_c - \hat{k}_1 + m_c)\gamma_\alpha}{((k_{\bar{c}} - k_3)^2 - m_c^2)((k_c - k_1)^2 - m_c^2)} + \frac{\gamma_\beta(-\hat{k}_{\bar{c}} + \hat{k}_2 + m_c)\gamma_\gamma(\hat{k}_c - \hat{k}_1 + m_c)\gamma_\alpha}{((k_{\bar{c}} - k_2)^2 - m_c^2)((k_c - k_1)^2 - m_c^2)} + \\ + \frac{\gamma_\gamma(-\hat{k}_{\bar{c}} + \hat{k}_3 + m_c)\gamma_\alpha(\hat{k}_c - \hat{k}_2 + m_c)\gamma_\beta}{((k_{\bar{c}} - k_3)^2 - m_c^2)((k_c - k_2)^2 - m_c^2)} + \frac{\gamma_\alpha(-\hat{k}_{\bar{c}} + \hat{k}_1 + m_c)\gamma_\gamma(\hat{k}_c - \hat{k}_2 + m_c)\gamma_\beta}{((k_{\bar{c}} - k_1)^2 - m_c^2)((k_c - k_2)^2 - m_c^2)} + \\ + \frac{\gamma_\beta(-\hat{k}_{\bar{c}} + \hat{k}_2 + m_c)\gamma_\alpha(\hat{k}_c - \hat{k}_3 + m_c)\gamma_\gamma}{((k_{\bar{c}} - k_2)^2 - m_c^2)((k_c - k_3)^2 - m_c^2)} + \frac{\gamma_\alpha(-\hat{k}_{\bar{c}} + \hat{k}_1 + m_c)\gamma_\beta(\hat{k}_c - \hat{k}_3 + m_c)\gamma_\gamma}{((k_{\bar{c}} - k_1)^2 - m_c^2)((k_c - k_3)^2 - m_c^2)}. \quad (48)$$

Note that equation (5) from ([101]) can be used to properly normalize the color wave function. If we take this into account, then the color wave function normalized to unity should have the following form:

$$\frac{1}{\sqrt{3}} \bar{q}_i q_i = \frac{1}{\sqrt{3}} (\bar{q}_1 q_1 + \bar{q}_2 q_2 + \bar{q}_3 q_3).$$

Here, the factor $1/\sqrt{3}$ ensures the correct normalization of this wave function.

It should be noted that the quantity ϕ in (46) is related to the charmonium wave function and can be written as follows:

$$\phi = \frac{|\psi(\mathbf{r} = \mathbf{0})|}{M_\psi^{3/2}} = \frac{\alpha_s^{3/2}}{3\sqrt{3\pi}}, \quad (49)$$

where α_s is the QCD coupling constant. Here the quantity ϕ is obtained from the decay rate of $\psi \rightarrow 3g$ on the mass shell. We understand that on the charmonium scale (for $s \sim M_c^2$) this three-gluon mechanism depends on its value to a rather high degree, and therefore, this mechanism, according to Eqs.(46) and (49), is very sensitive to this value of ϕ . For this process, when performing computations we use the value $\alpha_s(M_c) = 0.28$ which is expected at the QCD evolution of α_s from the b -quark scale to the c -quark scale, i.e., to $s \sim M_c^2$.

It should be noted that one of the most important corrections concerns the final state of $\Xi^0\bar{\Xi}^0$. During the execution of the process, after the decays of $\psi(3770)$, three gluons are obtained, then three more pairs of the quark-antiquark are formed and in the final state $\Xi^0\bar{\Xi}^0$ pairs are formed. To completely implement this mechanism, we need to reproduce the absolute value of the cross section. In this case, one of the goals of this mechanism is the transition of three gluons (i.e., with a total angular momentum of 1) into a final $\Xi^0\bar{\Xi}^0$ pair.

Based on the calculation method, we can assume that this mechanism has much in common in the time-like region with the production of $p\bar{p}$, $\Lambda\bar{\Lambda}$, $\Sigma^0\bar{\Sigma}^0$ and $\Sigma^+\bar{\Sigma}^-$ pairs from a photon [91–94]. In formula (46) we take the factor $G_\psi(s)$, describing the mechanism of the transition of three gluons into the final pair $\Xi^0\bar{\Xi}^0$, as a form factor. Thus, similar to (14), in (46) we can apply an additional form factor with a different value of the parameter C_ψ , that is

$$|G_\psi(s)| = \frac{C_\psi}{s^2 \log^2(s/\Lambda^2)}. \quad (50)$$

In the present reaction, for the parameter C_ψ we use the same value that was used in the case of the production of the $p\bar{p}$ and the $\Lambda\bar{\Lambda}$ [91, 92] pairs

$$C_\psi = (45 \pm 9) \text{ GeV}^4. \quad (51)$$

Now we need to restore the real part of Z_D from (33) and Z_{3g} from (47). By applying the technique of dispersion relations, which is described in detail in [90], we further obtain an expression for the real part of Z_D and Z_{3g} in the following form:

$$\text{Re } Z_i(\beta) = \frac{1}{\pi} \left\{ \text{Im } Z_i(\beta) \log \left| \frac{1 - \beta^2}{\beta_{\min}^2 - \beta^2} \right| + \int_{\beta_{\min}}^1 \frac{2\beta_1 d\beta_1}{\beta_1^2 - \beta^2} [\text{Im } Z_i(\beta_1) - \text{Im } Z_i(\beta)] \right\}. \quad (52)$$

When calculating the imaginary part, we made sure that the imaginary part $\text{Im } Z_D(\beta)$ of the contribution of the D - meson loop from (38) above the threshold ($s > 4M_D^2$) is not zero. So, this means that the integration over the lower limit in (52) is equal to $\beta_{\min} = \sqrt{1 - M_{\Xi}^2/M_D^2}$. However, we observe that when the value is $s_{\min} = 4M_{\Xi}^2$, the imaginary part $\text{Im } Z_{3g}(\beta)$ for the three-gluon contribution matches the reaction threshold, so we can treat the lower limit of integration as $\beta_{\min} = 0$.

VI. THE NUMERICAL RESULTS

Now in this section we want to describe the results we have obtained. We have studied in detail the characteristics of the distribution of the total cross section from the center-of-mass energy in electron-positron annihilations at BESIII energies [74]. In particular, according to our calculations, we have plotted the quantities of $Z_D(s)$ and $Z_{3g}(s)$ depending on the total energy \sqrt{s} in the range starting from the reaction threshold $s = 4M_{\Xi}^2$ to 4.95 GeV, since these quantities give the corresponding (D -meson loop and three gluons) contributions. Of course, we performed a comparison of all our theoretical results with the experimental data of BES III. Based on formula (13), we calculate the total cross section for the production of $\Xi^0\bar{\Xi}^0$ pairs in their annihilation process as a function of the collider center-of-mass energy in the range from 3.51 GeV to 4.95 GeV.

In Fig. 3, the dependence of the total cross section on the center-of-mass energy \sqrt{s} of the process $e^+e^- \rightarrow \Xi^0\bar{\Xi}^0$ in the Born approximation is presented.

We have plotted this graph based on the theoretical results for the total cross section in the Born approximation, and here our theoretical result is compared with the experimental BESIII data. It is seen that our result agrees well with the experimental points. It should also be noted that the maximum value of the total cross-section is obtained at an energy of $\sqrt{s} = 3.51$ GeV, then, with increasing energy, the total cross-section smoothly decreases.

Note that the propagator between the vertices of $D^0\bar{D}^0$ contains five types of hyperons – Σ_c^0 , Σ^0 , Λ^0 , Ω_c^0 , Ξ_c^0 , i.e., there are different options in this reaction. Of course, the hyperons formed in the final state can be obtained from different combinations of quarks. When our calculations we used the average mass of five hyperons for the hyperon mass in the propagator (between the vertices of $D^0\bar{D}^0$).

Figure 6 shows the dependence of the quantity of $Z_D(s)$ on the total energy \sqrt{s} in the

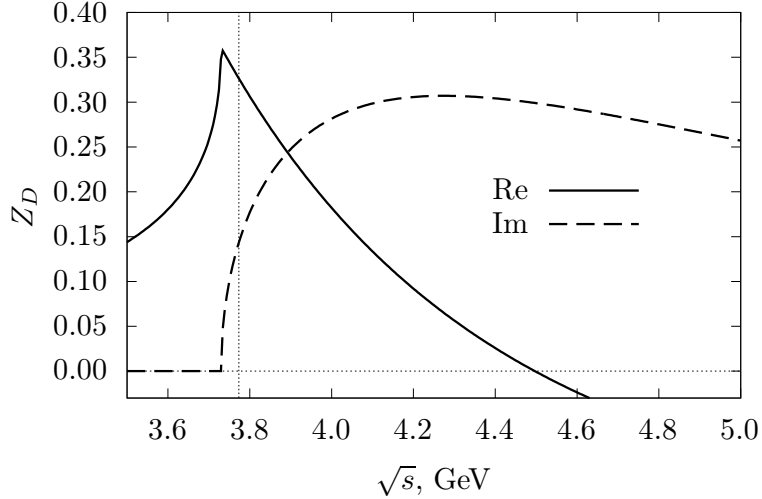


Figure 6: The quantity $Z_D(s)$ from (33) depending on the center-mass-energy \sqrt{s} starting from the threshold $\sqrt{s} = 2M_{\Xi}^0$. The position of $\psi(3770)$ is indicated by a vertical dashed line.

range from the reaction threshold $\sqrt{s} = 2M_{\Xi}^0$ to 4.95 GeV. The form and numerical values of the real and imaginary parts of this quantity are almost the same as in the cases of the production of proton-antiproton (see Fig. 7(a) in [91]), $\Lambda\bar{\Lambda}$ [Fig. 6 in [92]], and $\Sigma^0\bar{\Sigma}^0$ [Fig. 6 in [93]] and $\Sigma^+\bar{\Sigma}^-$ [Fig. 6 in [94]]. Figure 7 presents the dependence of the real and imaginary parts of $Z_{3g}(s)$ on the total energy \sqrt{s} in the range from the reaction threshold $\sqrt{s} = 2M_{\Xi}^0$ to 4.95 GeV.

It can be seen from the graph that the general behavior of the $Z_{3g}(s)$ curves in \sqrt{s} is very different from the curves that were obtained in the case of the production of proton-antiprotons [Fig. 7 (B) [91]], $\Lambda\bar{\Lambda}$ [Fig. 7 [92]], and $\Sigma^0\bar{\Sigma}^0$ [Fig. 7 in [93]], but it shows a similar general behavior of the curves as in the case of the $\Sigma^+\bar{\Sigma}^-$ final state (Fig. 7 in [94]). Nevertheless, it can be seen from the graph that the characteristic large negative quantity of $Z_{3g}(s)$ still remains the same, since it gives a large relative phase with respect to the Born contribution in the amplitude. Taking into account the above, we can make sure that the quantities $Z_D(s)$ from (33) and $Z_{3g}(s)$ from (47) are considered to be the main parts of the total cross section that give the corresponding contributions (D -meson loop and trigluons). In Figs.6 and 7, the resonance position $\psi(3770)$ is marked with a vertical dotted line. The theoretical results for the contribution of the D -meson loop to the Born cross section are presented in Fig.8. Similarly, in Fig.9 we show the result of the three-gluon contribution to

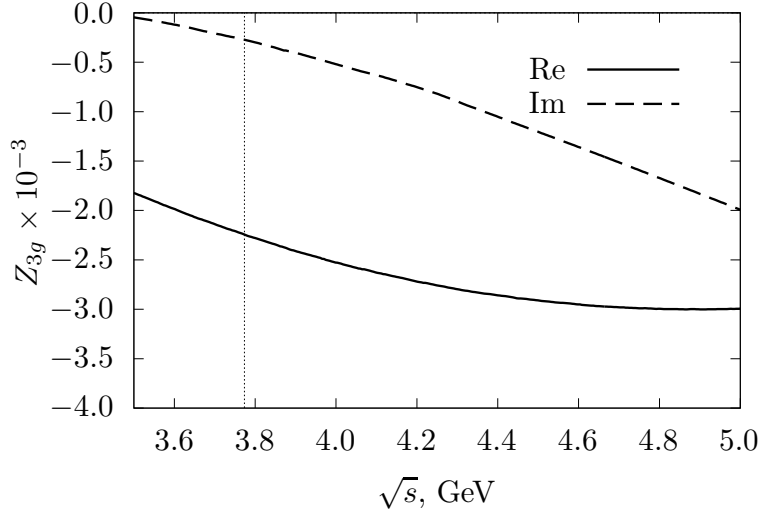


Figure 7: The quantity $Z_{3g}(s)$ from (47) depending on the center-mass-energy \sqrt{s} starting from the threshold $\sqrt{s} = 2M_{\Xi}^0$. The position of $\psi(3770)$ is indicated by a vertical dashed line.

the Born cross section. Our theoretical results, which we show in Figs.8 and 9 for both of these contributions, are compared with the experimental data of the BESIII collaboration [74].

From Fig. 8 we see that the experimental point at $\sqrt{s} = 3770$ GeV, i.e., the charmonium resonance point $\psi(3770)$, almost coincides with our theoretical results. The cross-section for the contribution of the three-gluon mechanism, which is presented in Fig. 9, shows that the experimental result at the point $\sqrt{s} = 3770$ GeV, i.e., the charmonium resonance point $\psi(3770)$, completely coincides with our theoretical result. Finally, we have studied the total cross section taking into account both contributions, i.e., the D -meson loop and the three-gluon mechanism, which we show in Fig. 10, and from this it can be seen that the experimental result at the charmonium resonance point $\psi(3770)$ completely coincides with our theoretical result.

The theoretical results of the total cross-section obtained by us in the energy range $\sqrt{s} = 3.5 - 5.0$ GeV by taking into account the contributions of the D -meson loop and three-gluon mechanisms in the Born cross-section and comparisons with the BESIII [74] data are shown in Fig. 10. We would like to note that the peak is near the resonance $\psi(3770)$ of charmonium and is clearly visible, which can be seen from this graph. According to our model, we mainly consider the $\psi(3770)$ vicinity. In addition, for the reaction $e^+e^- \rightarrow \Xi^0\bar{\Xi}^0$, we study the

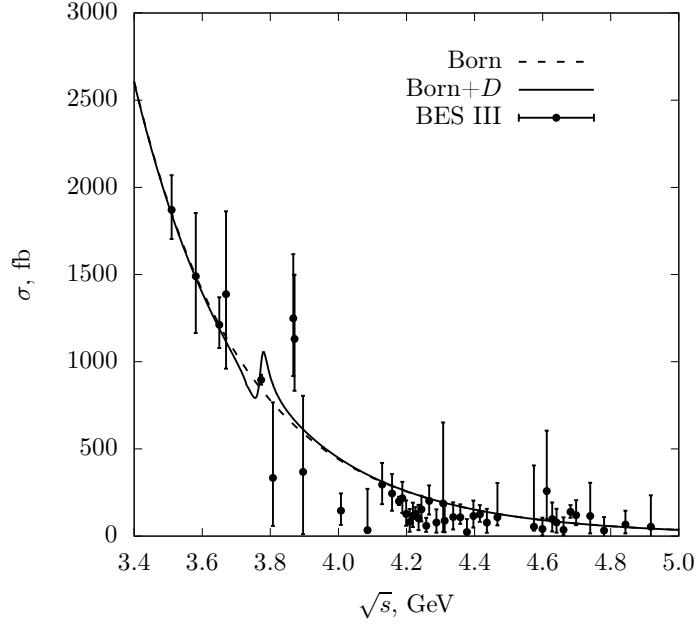


Figure 8: Total cross section distributions of the process $e^+e^- \rightarrow \Xi^0\bar{\Xi}^0$ as a function of the center-of-mass energy \sqrt{s} with the inclusion of the D -meson loop contributing. The Experimental data are from BESIII Collaboration [74].

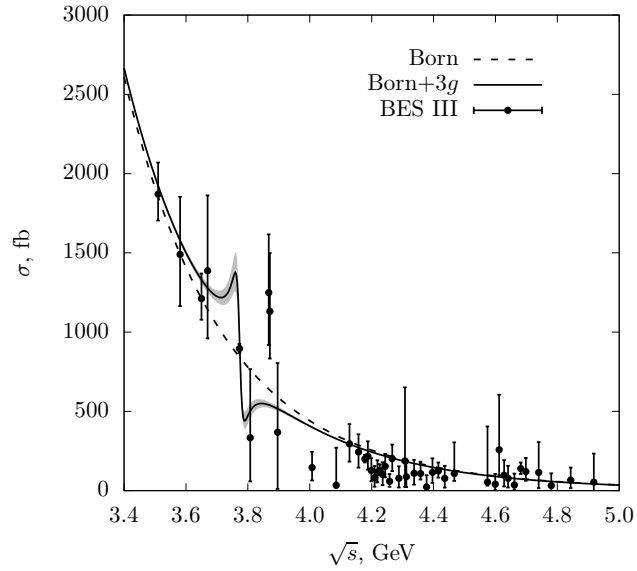


Figure 9: The total cross section distributions of the process $e^+e^- \rightarrow \Xi^0\bar{\Xi}^0$ as a function of the center-of-mass energy \sqrt{s} with the inclusion of three-gluons contributing. The Experimental data are from BESIII Collaboration [74].

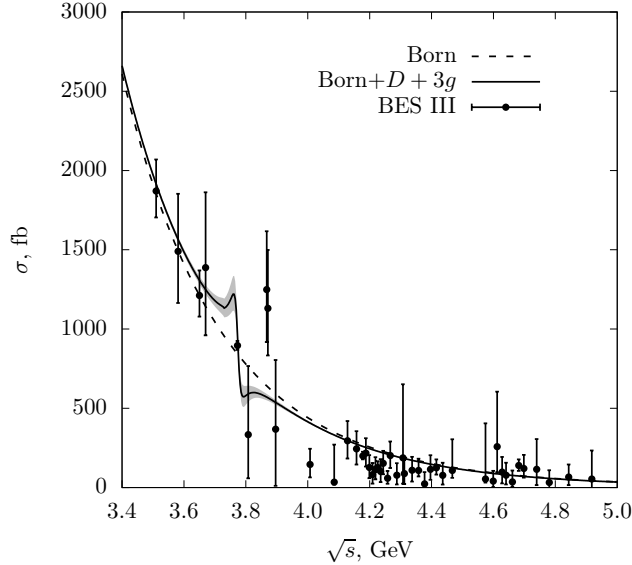


Figure 10: The total cross section distributions of the process $e^+e^- \rightarrow \Xi^0\bar{\Xi}^0$ as a function of the center-of-mass energy \sqrt{s} including two mechanisms (D -meson loop and three gluon). The Experimental data are from BESIII Collaboration [74].

vicinity with new charmonium-like states in the same energy region, for example, $\psi(4040)$, $\psi(4160)$, $Y(4230)$, $Y(4360)$, $\psi(4415)$, and $Y(4660)$. It should be noted that we have the $\psi(3770)$ charmonium in the intermediate state, but besides that, we compute and investigate the total cross section of this process taking into account new charmonium-like states in the intermediate state.

Recall that in the process we are looking at, $e^+e^- \rightarrow \Xi^0\bar{\Xi}^0$, we do not make any additional parameter fitting; instead, we keep all the necessary parameters of our model the same as in the process $e^+e^- \rightarrow p\bar{p}$ [91].

Now we can determine the total relative phase ϕ_ψ of the charmonium contribution \mathcal{M}_ψ to the amplitude relative to the Born contribution \mathcal{M}_B without taking into account the Breit-Wigner factor, i.e.:

$$S_D(s) + S_{3g}(s) = |S(s)|e^{i\phi_\psi}, \quad (53)$$

where $S_D(s)$ was defined in (32) and $S_{3g}(s)$ is from (45). The dependence of the total relative phase ϕ_ψ on the energy of the center of mass \sqrt{s} is plotted in Fig. 11. Here we also want to note that in this figure the resonance position of the $\psi(3770)$ charmonium is also marked with a vertical dashed line. As can be seen from Fig. 11, at the point $\psi(3770)$

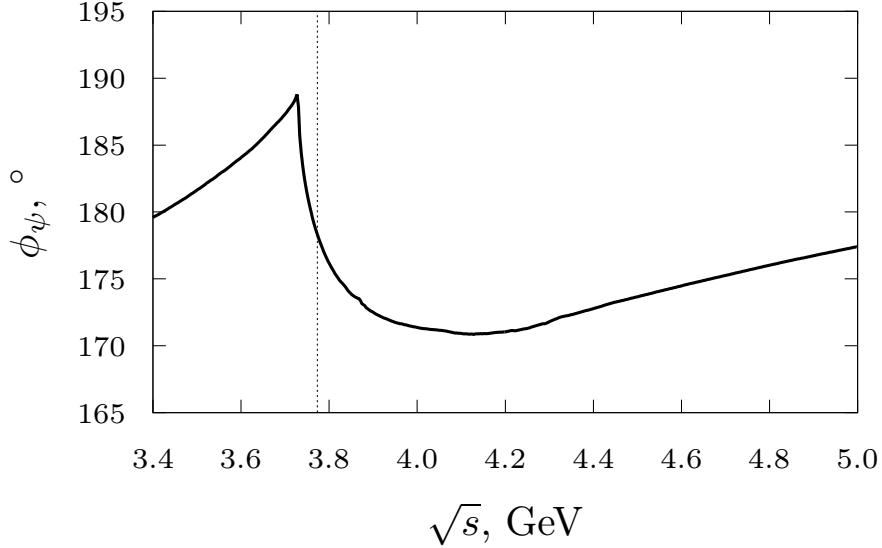


Figure 11: The dependence of the relative phase of the charmonium $\psi(3770)$ contribution from the total invariant energy \sqrt{s} .

of charmonium, the relative phase and the corresponding total cross section (20) have the following value

$$\sigma_\psi = 1005.75 \text{ fb}, \quad \phi_\psi = 178.45^\circ. \quad (54)$$

It can be concluded that for the decay of charmonium into two baryons to the finite state, such a property is common. This has been also shown in [90–92], for decay of the charmonium $\psi(3770)$ into a pair $p\bar{p}$ and a pair $\Lambda\bar{\Lambda}$, and the $\chi_{c2}(1P)(3556)$ charmonium in [95].

In this paper, for the $\Xi^0\bar{\Xi}^0$ production in the e^+e^- annihilation process, in addition to the contribution of the $\psi(3770)$ charmonium in the intermediate state, we also investigated the contributions from charmonium-like states, $\psi(4040)$, $\psi(4160)$, $Y(4230)$, $Y(4360)$, $\psi(4415)$, and $Y(4660)$. For the process $e^+e^- \rightarrow \Xi^0\bar{\Xi}^0$ we plotted the total cross section as a function of the total energy of the collider in the region of $\sqrt{s} = 3.51 - 4.95$ GeV based on the results of the contributions of charmonium-like states, i.e., respectively for $\psi(4040)$, $\psi(4160)$, $Y(4230)$, $Y(4360)$, $\psi(4415)$ and $Y(4660)$, and we presented them in Fig. 12. We are pleased to note that at the point for each resonance of the charmonia $\psi(4040)$, $\psi(4160)$, $Y(4230)$, $Y(4360)$, $\psi(4415)$, and $Y(4660)$, the experimental result agrees well with our theoretical result, which can be seen in Fig. 12.

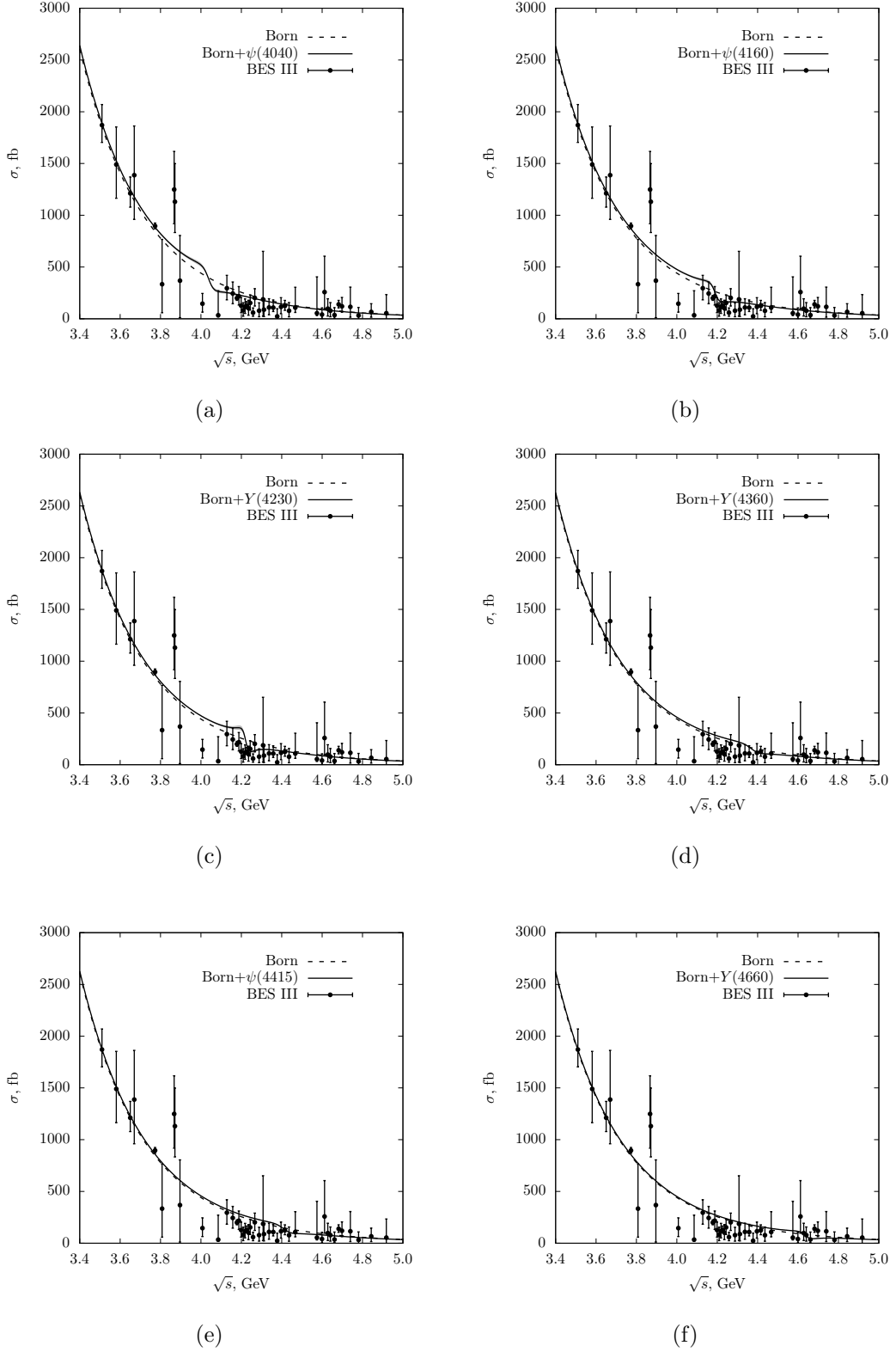


Figure 12: The total cross section distributions of the process $e^+e^- \rightarrow \Xi^0\bar{\Xi}^0$ as a function of the center-of-mass energy \sqrt{s} for the contribution of charmonium (-like) states, $\psi(4040)$, $\psi(4160)$, $Y(4230)$, $Y(4360)$, $\psi(4415)$, and $Y(4660)$. Experimental data are from BESIII Collaboration [74].

VII. DISCUSSION AND CONCLUSION

We have investigated the production of $\Xi^0\bar{\Xi}^0$ pairs in the process of e^+e^- annihilation in the vicinity of the charmonium resonance $\psi(3770)$ at the center-of-mass energy from 3.51 to 4.95 GeV collected with the BESIII detector at the BEPCII collider and corresponding to an integrated luminosity of 30 fb^{-1} . It is worth noting that we have also investigated this process near other charmonia, i.e., with new charmonium-like states, for example, $\psi(4040)$, $\psi(4160)$, $Y(4230)$, $Y(4360)$, $\psi(4415)$, and $Y(4660)$, in the same energy region. We studied the production of $\Xi^0\bar{\Xi}^0$ pairs in the process of e^+e^- annihilation at the first stage within the framework of QED in the Born approximation. In addition to the Born mechanism, we also studied the total cross sections taking into account two more contributions associated with the intermediate state of the $\psi(3770)$ charmonium and other new charmonium-like states, for example, $\psi(4040)$, $\psi(4160)$, $Y(4230)$, $Y(4360)$, $\psi(4415)$, and $Y(4660)$. One of these contributions is a D -meson loop and the second contribution is the three-gluon mechanism. We compared the theoretical results obtained with the experimental data of the BESIII [74]. It should be noted that their total sum gives a rather good agreement with the experimental point at $\sqrt{s} = M_{\psi, Y}$. We have already mentioned that the process $e^+e^- \rightarrow \Xi^0 + \bar{\Xi}^0$ can also be implemented by the vector charmonium state $\psi(3770)$ as well as by other charmonium-like states. Let us note that the photon, ψ , and other charmonium-like states are vector mesons; therefore, the structures of the cross-section distributions were similar.

Indeed, in this $e^+e^- \rightarrow \Xi^0 + \bar{\Xi}^0$ process both mechanisms make a significant contribution, and they explain the main part of the final result. In turn, one of the important results is that the curve we obtained reproduces the tendency of the experimental points in the left and right shoulders relative to the central point. When performing computations in this process, we did not use any procedures for fitting. For this purpose, all necessary parameters were used fixed for the $p\bar{p}$ production channel in [91]. We aimed to implement a fine scan with small steps of the energy area around the charmonium resonance $\psi(3770)$.

Hence we can draw a solid conclusion that in this work, as in other works, in the charmonium decay the vertex phases $\psi \rightarrow p\bar{p}$, $\psi \rightarrow \Lambda\bar{\Lambda}$, $\psi \rightarrow \Sigma^0\bar{\Sigma}^0$, $\psi \rightarrow \Sigma^+\bar{\Sigma}^-$ and $\psi \rightarrow \Xi^0\bar{\Xi}^0$ are large ($\phi_\psi \sim 200^\circ$) and can be measured accurately in these channels. It is to be noted that the generation of a large phase for the production of a hyperon pair in the e^-e^+ annihilation process was shown in the present work and in a series of other works [90–95]. Finally,

in conclusion, we intend to report that in the future we plan also to consider other binary processes of final state formation activated by charmonium annihilation.

VIII. ACKNOWLEDGEMENTS

I am grateful to Dr. Yu. M. Bystritskiy for useful discussions.

IX. DATA AVAILABILITY

The data that support the findings of this article are openly available [74].

-
- [1] S. L. Glashow, Nucl. Phys. B22 (1961)579.
 - [2] S. Weinberg, Phys. Rev. Lett. 19 (1967)1264.
 - [3] A. Salam, Elementary Particle Theory. Stockholm, 1968, p. 367.
 - [4] A. Salam, J.C. Ward, Phys.Lett. 13 (1964)168.
 - [5] X. Liu, Chin. Sci. Bull. 59, 3815 (2014), arXiv:1312.7408 [hep-ph].
 - [6] H.-X. Chen, W. Chen, X. Liu, and S.-L. Zhu, Phys. Rept. 639, 1 (2016), arXiv:1601.02092 [hep-ph].
 - [7] H.-X. Chen, W. Chen, X. Liu, Y.-R. Liu, and S.-L. Zhu, Rept. Prog. Phys. 80, 076201 (2017), arXiv:1609.08928 [hep-ph].
 - [8] F.-K. Guo, C. Hanhart, U.-G. Meißner, Q. Wang, Q. Zhao, and B.-S. Zou, Rev. Mod. Phys. 90, 015004 (2018), [Erratum: Rev.Mod.Phys. 94, 029901 (2022)], arXiv:1705.00141 [hep-ph].
 - [9] Y.-R. Liu, H.-X. Chen, W. Chen, X. Liu, and S.-L. Zhu, Prog. Part. Nucl. Phys. 107, 237 (2019), arXiv:1903.11976 [hep-ph].
 - [10] N. Brambilla, S. Eidelman, C. Hanhart, A. Nefediev, C.-P. Shen, C. E. Thomas, A. Vairo, and C.-Z. Yuan, Phys. Rept. 873, 1 (2020), arXiv:1907.07583 [hep-ex].
 - [11] H.-X. Chen, W. Chen, X. Liu, Y.-R. Liu, and S.-L. Zhu, Rept. Prog. Phys. 86, 026201 (2023), arXiv:2204.02649 [hep-ph].
 - [12] M. Ablikim et al. (BESIII), Chin. Phys. C 44, 040001 (2020), arXiv:1912.05983 [hep-ex].
 - [13] B. Aubert et al. (BaBar Collab.), Phys. Rev. Lett. 95, 142001 (2005).

- [14] C. Z. Yuan *et al.* (Belle Collab.), *Phys. Rev. Lett.* **99**, 182004 (2007).
- [15] Q. He *et al.* (CLEO Collaboration), *Phys.Rev. D* **74**, 091104(R) (2006).
- [16] B. Aubert *et al.* (BaBar Collab.), *Phys. Rev. Lett.* **98**, 212001 (2007).
- [17] X. L. Wang *et al.* (Belle Collab.), *Phys. Rev. Lett.* **99**, 142002 (2007).
- [18] J.P. Lees *et al.* (BABAR Collaboration), *Phys.Rev. D*, **89**, 111103 (2014).
- [19] X.L. Wang *et al.* (Belle Collaboration), *Phys.Rev. D*, **91**, 112007 (2015).
- [20] S. J. Brodsky and G. P. Lepage, *Phys. Rev. D* **24**, 2848 (1981).
- [21] N. G. Stefanis and M. Bergmann, *Phys. Lett. B* **304**, 24 (1993).
- [22] J. Bolz and P. Kroll, *Eur. Phys. J. C* **2**, 545 (1998).
- [23] M. Ablikim *et al.* (BESIII Collaboration), *Phys. Rev. D* **87**, 032007 (2013).
- [24] M. Ablikim *et al.* (BESIII Collaboration), *Phys. Lett. B* **770**, 217-225 (2017).
- [25] M. Ablikim *et al.* (BESIII Collaboration), *Phys. Rev. D* **93**, 072003 (2016).
- [26] X. F. Wang, B. Li, Y. N. Gao and X. C. Lou, *Nucl. Phys. B* **941**, 861-867 (2019).
- [27] M. Ablikim *et al.* (BESIII Collaboration), *Phys. Rev. D* **99**, 032006 (2019).
- [28] N. Brambilla *et al.* (Quarkonium Working Group), arXiv:hep-ph/0412158.
- [29] R. Frisch, O. Stern, *Z. Phys.* **85**, 4 (1933).
- [30] R. Hofstadter, *Rev. Mod. Phys.* **28**, 214 (1956).
- [31] G. Eichmann, H. Sanchis-Alepuz, R. Williams, R. Alkofer, C.S. Fischer, *Prog. Part. Nucl. Phys.* **91**, 1 (2016).
- [32] G. Ramalho, K. Tsushima, A.W. Thomas, *J. Phys. G* **40**, 015102 (2013).
- [33] F. Gross, G. Ramalho, K. Tsushima, *Phys. Lett. B* **690**, 183 (2010).
- [34] G. Ramalho, M.T. Peña, K. Tsushima, Myung-Ki Cheoun, *Phys. Lett. B* **858**, 139060 (2024).
- [35] G. Ramalho, M.T. Peña, K. Tsushima, *Phys. Rev. D* **101**, 014014 (2020).
- [36] L.S. Geng, J. Martin Camalich, L. Alvarez-Ruso, M.J. Vicente Vacas, *Phys. Rev. Lett.* **101**, 222002 (2008).
- [37] S.J. Brodsky, G.R. Farrar, *Phys. Rev. D* **11**, 1309 (1975).
- [38] J.R. Green, J.W. Negele, A.V. Pochinsky, S.N. Syritsyn, M. Engelhardt, S. Krieg, *Phys. Rev. D* **90**, 074507 (2014).
- [39] M. Ablikim, M.N. Achasov, P. Adlarson, S. Ahmed, M. Albrecht, R. Aliberti, A. Amoroso, M.R. An, Q. An, X.H. Bai *et al.*, *Phys. Rev. D* **105**, L011101 (2020).
- [40] B. Delcourt *et al.*, *Phys. Lett.* **86B**, 395 (1979).

- [41] A. Antonelli *et al.*, Nucl. Phys. **B517**, 3 (1998).
- [42] T. A. Armstrong *et al.*, Phys. Rev. Lett, **70**, 1212 (1993).
- [43] T. K. Pedlar *et al.*, Phys. Rev. Lett, **95**, 261803 (2005).
- [44] M. Ablikim *et al.*, Phys. Rev. Lett, **120**, 132001 (2018).
- [45] R. Hofstadter, R.W. McAllister, Phys. Rev. **98**, 217 (1955).
- [46] R. Hofstadter, R.W. McAllister, Phys. Rev. **102**, 851 (1956).
- [47] X. L. Wang *et al.* (Belle Collaboration), Phys. Rev. D **87**, 051101(R) (2013).
- [48] W. Bacino *et al.* (DELCO Collaboration), Phys. Rev. Lett. **40**, 671 (1978).
- [49] S. Godfrey and Isgure, Phys. Rev. D **32**, 189 (1985).
- [50] N. Brambilla *et al.*, Eur. Phys. J. C **71**, 1534 (2011).
- [51] R.A. Briceno *et al.*, Chin. Phys. C **40**, 042001 (2016).
- [52] J. Haidenbauer, X.W. Kang, and U.G. Meißner, Nucl.Phys. **A929**, 102 (2014);
arXiv:1405.1628 [nucl-th].
- [53] A. Bianconi, E. Tomasi-Gustafsson, Phys. Rev. C **93**, 035201 (2016); arXiv:1510.06338
[nucl-th]. doi:10.1103/PhysRevC.93.035201
- [54] Qin-He Yang, Di Guo, Ling-Yun Dai, Johann Haidenbauer, Xian-Wei Kang, Ulf-G. Meißner,
Sci. Bull. **68**, 2729 (2023); arXiv:2206.01494 [nucl-th].
- [55] A.I. Milstein, S.G. Salnikov, Phys. Rev. D **106**, 074012 (2022); arXiv: 2207.14020 [hep-ph].
- [56] N. Cabibbo and R. Gatto, Phys. Rev. Lett. **4**, 313 (1960).
- [57] N. Cabibbo and R. Gatto, Phys. Rev. **124**, 1577 (1961).
- [58] M. Ablikim, M.N. Achasov, P. Adlarson, S. Ahmed, M. Albrecht, R. Aliberti, A. Amoroso,
M.R. An, Q. An, X.H. Bai *et al.*, Phys. Rev. D **105**, L011101 (2020).
- [59] M. Ablikim *et al.*, (BESIII Collaboration), Phys. Rev. D **104**, L091104 (2021).
- [60] M. Ablikim *et al.*, (BESIII Collaboration), Phys. Rev. D **97**, 032013 (2018).
- [61] M. Ablikim *et al.*, (BESIII Collaboration), Phys. Lett. B **735**, 101 (2014).
- [62] B. Aubert *et al.*, (BABAR Collaboration), Phys. Rev. D **76**, 092006 (2007).
- [63] J.P. Lees *et al.*, (BABAR Collaboration), Phys.Rev. D **87**, 092005 (2013).
- [64] J.P. Lees *et al.*, (BABAR Collaboration), Phys.Rev. D **88**, 072009 (2013).
- [65] M. Ablikim *et al.*, (BESIII Collaboration), Phys.Rev. D **91**, 112004 (2015).
- [66] G.P. Lepage and S.J. Brodsky, Phys.Rev.Lett. **43**, 545 (1979), [Erratum: Phys.Rev.Lett. **43**,
1625 (1979)]. doi:10.1103/PhysRevLett.43.1625.2

- [67] A.V. Belitsky, X.d. Ji, and F. Yuan, *Phys.Rev.Lett.* **91**, 092003 (2003).
- [68] D.M. Asner *et al.*, *Int. J. Mod. Phys. A* **24**, 499 (2009).
- [69] M. Ablikim *et al.* (BESIII Collaboration), *Chin. Phys. C* **39**, 093001 (2015).
- [70] M. Ablikim *et al.* (BESIII Collaboration), *Phys.Rev. D* **103**, 012005 (2021)
- [71] M. Ablikim *et al.* (BESIII Collaboration), *Phys.Lett. B* **831**, 137187 (2022)
- [72] M. Ablikim *et al.* (BESIII Collaboration), *JHEP* 11, **228** (2023)
- [73] M. Ablikim *et al.* (BESIII Collaboration), *JHEP* 05, **022** (2024)
- [74] M. Ablikim *et al.* (BESIII Collaboration), *JHEP* 11, **062** (2024)
- [75] P.A. Rapidis, *et al.*, *Phys. Rev. Lett.* **39**, 526 (1978). doi:10.1103/PhysRevLett.39.526
- [76] D. Pallin *et al.*, (DM2 Collaboration), *Nucl. Phys.* **B292**, 653 (1987).
- [77] S. Navas *et al.*, (Particle Data Group), Review of particle physics, *Phys. Rev. D* 110, 030001 (2024).
- [78] L. Kopke, N. Wermes, *Phys. Rep.* **174**, 67 (1989).
- [79] M. Ablikim *et al.*, (BESIII Collaboration), *Phys. Lett. B* **814**, 136110 (2021).
- [80] M. Ablikim *et al.*, (BESIII Collaboration), *Phys.Lett. B* **820**, 136557 (2021).
- [81] M. Ablikim *et al.*, (BESIII Collaboration), *Phys.Lett. B* **770**, 217 (2017).
- [82] M. Ablikim *et al.*, (BESIII Collaboration), *JHEP* 06, **074** (2022).
- [83] S. Dobbs, A. Tomaradze, T. Xiao, K.K. Seth, G. Bonvicini, *Phys. Lett. B* **739**, 90 (2014).
- [84] S. Dobbs, K.K. Seth, A. Tomaradze, T. Xiao, and G. Bonvicini, *Phys. Rev. D* **96**, 092004 (2017).
- [85] Xiongfei Wang, (on behalf of BESIII Collaboration), *Proc.Sci.*, CHARM2020 026.
- [86] E. Tomasi-Gustafsson, A. Bianconi, and S. Pacetti, *Phys. Rev. C* **103**, 035203 (2021).
- [87] R.B. Ferroli, S. Pacetti, and A. Zallo, *Eur.Phys.J. A* **48**, 33 (2012).
- [88] G. Lepage and S. J. Brodsky, *Phys. Rev. D* **22**, 2157 (1980).
- [89] A. Amoroso *et al.*, *Universe* **7**, 436 (2021).
- [90] A.I. Ahmadov, Yu. M. Bystritskiy, E.A. Kuraev, and P. Wang, *Nucl. Phys.* **B888**, 271 (2014).
- [91] Yu.M. Bystritskiy, *Phys. Rev. D* **103**, 116029 (2021).
- [92] Yu.M. Bystritskiy, A.I. Ahmadov, *Phys. Rev. D* **105**, 116012 (2022).
- [93] A.I. Ahmadov, *Phys. Rev. D* **109**, 096037 (2024).
- [94] A.I. Ahmadov, *Phys. Rev. D* **111**, 056008 (2025).

- [95] E. Kuraev, Y. Bystritskiy, and E. Tomasi-Gustafsson, Nucl. Phys. **A920**, 45 (2013).
- [96] G. Gong *et al.*, (BELLE Collaboration), Phys. Rev. D **107**, 072008 (2023); arXiv: 2210.16761 [hep-ex].
- [97] R. E. Cutkosky, Rev. Mod. Phys. **33**, 448 (1961).
- [98] F. Navarra and M. Nielsen, Phys. Lett. B **443**, 285 (1998).
- [99] L. Reinders, H. Rubinstein, and S. Yazaki, Phys.Rep. **127**, 1 (1985).
- [100] Seungho Choe, Phys. Rev. C **57**, 2061 (1998).
- [101] H. Chiang, J. Hufner, H. Pirner, Phys. Lett. B **324**, 482 (1994).